ANNALI DI GEOFISICA, VOL. XXXVII, N. 1, April 1994

Long-period *P* waveform modeling of upper mantle phases in the West Mediterranean basin

Nicola Alessandro Pino
Istituto Nazionale di Geofisica, Roma, Italy

Abstract
Long-period *P* waveforms of some Italian crustal earthquakes recorded at the WWSSN stations located in the Iberian Peninsula have been modeled to derive a 1-*D* upper mantle compressional velocity model. A technique based on the Cagniard-de Hoop method has been used to compute synthetic seismograms. Waveforms have first been computed for published velocity models referred to different tectonic provinces and compared with the data. A model that strongly improves the fits to the data is then presented. The proposed model, called WMP, is characterized by a 100 km thick lid overlaying a low velocity zone, a 1% velocity discontinuity located at 313 km depth, that is required to fit a lower amplitude phase, and an abrupt increase in the velocity gradient starting from 370 km. This latter is preferred to the sharp discontinuity located at about 400 km that is present in various models obtained for upper mantle structure with analogous techniques. Within the lid and the low-velocity zone, WMP displays features that are typical of old ocean structures like the Northwest Atlantic Ocean.

Key words *upper mantle – West Mediterranean – waveform modeling*

1. Introduction

In the last fifteen years there has been much interest in the upper mantle structure and its lateral variations. Understanding the nature of the Earth's structure down to 700 km is crucial to a full comprehension of processes like mantle convection and sea-floor spreading. The problem of the depth to which continents act as coherent plates during continental drift, originally addressed by MacDonald (1963), is still open. The determination of the seismic structure may help in constraining mantle's composition and dynamic behavior. For instance Hager (1984) used the topography of mantle discontinuities to constrain the depth of mantle convection, Anderson and Bass (1984) computed seismic velocities for different petrological models, Duffy and Anderson (1989) and Ita and Stixrude (1992) used the V_p/V_s ratio to derive information on mineralogy.

The Mediterranean region is characterized by a highly complex tectonic environment as testified by the surface geology and the seismicity pattern; although the general geodynamic frame has been understood, there are still several open questions which are strongly debated by geophysicists and geologysts.

Many seismological studies on the upper mantle structure in the European-Mediterranean area have been done using different approaches. In particular, tomographic models have been obtained from teleseismic (*e.g.* Romanowicz, 1980) and from regional and teleseismic (Spakman, 1991) *P* wave travel times and, at smaller scale,

travel time tomography has been performed for particularly interesting areas, such as the Hellenic subduction zone (Spakman *et al.*, 1988) or the Italian region (Scarpa, 1982; Amato *et al.*, 1993); studies utilizing surface waves have been done by Cara *et al.* (1980), Panza *et al.* (1980), Marillier and Mueller (1985) and Snieder (1988); body wave travel time data have been modeled by several authors, especially in the continental European area (Payo, 1969; Mayer-Rosa and Mueller, 1973; England and Worthington, 1977), and only in a few cases techniques of matching either long-period (Burdick, 1981) or broad-band (Paulssen, 1987) body waveforms with synthetic seismograms have been applied.

Tomographic studies are especially suitable to provide maps of relative velocity but they require a high density of both earthquakes and stations. Moreover, due to the ray paths, the vertical resolution in the upper mantle is usually on the order of 100 km at their best. On the other hand only travel times are utilized. Surface wave studies, dispersion analysis and waveform inversion have even lower resolution.

Forward modeling is a largely applied method for interpreting the different seismic phases and for determining the absolute values of seismic velocities. This technique allows a direct control of the effects that different structural features produce on the waveforms. Once the model space has been extensively explored to determine the gross structure, this can be refined by finely fitting the waveforms and an investigation of the small scale heterogeneities is then possible.

In the last decade, several upper mantle models for different regions have been obtained by matching body waveforms from regional earthquakes with synthetic seismograms in horizontally stratified media (*e.g.* Grand and Helmberger, 1984; Walck, 1984; LeFevre and Helmberger, 1989; Zhao and Helmberger, 1993). As long as paths entirely belonging to the same tectonic province (pure paths) are considered, the resulting model may represent a reliable image of the actual velocity distribution. However, even if laterally inhomogeneous structures are analysed, this approach can provide information on the degree of lateral heterogeneity (Paulssen, 1987).

In this paper, modeling of some *P* waveforms from WWSSN-LP regional recordings of upper mantle phases for the West Mediterranean area is presented. A preliminary analysis has been performed by computing synthetic seismograms for published compressional velocity models obtained in different tectonic regions. A final model has then been determined through a trial-and-error approach.

2. Data

Upper mantle structure produces triplications on *P* phases at distances up to 30°; first arrivals up to 17° correspond to rays bottoming in the uppermost 400 km, for tectonic structures as well as for shield ones (Burdick, 1981). At distances closer than 10°, *P* wavetrains are dominated by the longer-period *PL* phase which can contaminate seismograms (Helmberger, 1972). In order to model the uppermost 400 km structure of the mantle, data recorded in the range 12°-17° should then be considered. Magnitude of earthquakes should be large enough to produce a high signal to noise ratio, larger than $M = 5$ for this distance range, but not much larger, if one wants to deal with point-like sources and to avoid source complexities (finiteness of fault plane, directivity, complex source time function, etc.) that can considerably affect waveforms.

Due to the stations and seismicity distributions in the West Mediterranean basin, WWSSN-LP stations located in the Iberian Peninsula have been considered for this study. Among the 5.0-6.0 magnitude Italian earthquakes in the period 1977-1990, the best recorded events have been selected (table I). Figure 1 shows the location of stations and events selected for this study; the

Table I. Earthquakes.

Event	Date	h	min	s	Latitude	Longitude	Depth	m_b
1	790919	21	35	37.2	42.812	13.061	16.	5.9
2	791208	4	6	34.3	38.284	11.741	33.	5.4
3	800528	19	51	19.3	38.482	14.252	12.	5.7
4	801125	18	28	21.5	40.660	15.450	15.	4.9
5	840507	17	49	41.6	41.765	13.898	10.	5.5

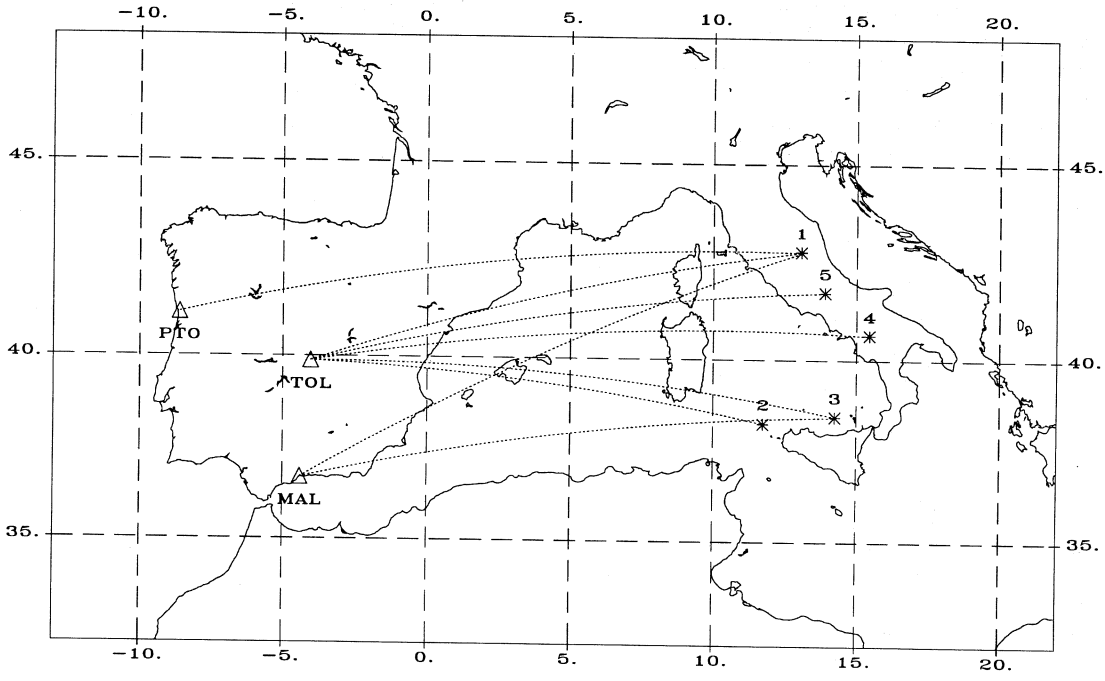

Fig. 1. Map showing the studied area with event (stars) and station (triangles) locations. Source-to-receiver great circle paths are also shown.

source-to-receiver great circle paths are also shown. All the events are located in the crust along the tectonic margin between the African and European plates; three of them occurred in the Apennines range (1, 4, 5), one was located west of Sicily (2) and one (3) occurred in the Southern Tyrrhenian Sea, where the seismicity pattern displays events located from 0 km to 500 km depth, with a continuous trend. This feature has been connected to a NW dipping slab by several authors (*e.g.* Anderson and Jackson, 1987a).

3. Modeling technique

Synthetic seismograms have been obtained by convolution of several factors according to the relation:

$$Y(t) = S(t) * I(t) * A(t) * G(t) \qquad (3.1)$$

where $S(t)$ is the «effective source» operator, $I(t)$ is the instrument response, $A(t)$ accounts for the anelastic attenuation and $G(t)$ is the Green's function. The operator S includes the source parameters (mechanism and source time function) and the free surface reflections *pP* and *sP*. Source parameters for all the modeled events, except for event 4, have been obtained by Anderson and Jackson (1987b). They used first-motion polarities and teleseismic waveform modeling to determine fault-plane solutions. Their focal mechanisms have been assumed except for cases where a clear first pulse polarity misfit resulted between synthetics and data. Epicentral locations, origin times and focal depths (from Anderson and Jackson, 1987b) are those reported by the International Seismological Centre (ISC) when available, otherwise those from the National Earthquake Information Service (NEIS) of the United States Geological Survey (USGS) have been used. For the event 4, not included in the Anderson and Jackson's study, the NEIS location and the source mechanism from the CMT catalogue have been considered. In most cases the focal depth has been moved in order to fit the *P* to *pP* relative timing. However, the determination of source parameters is not part of this study.

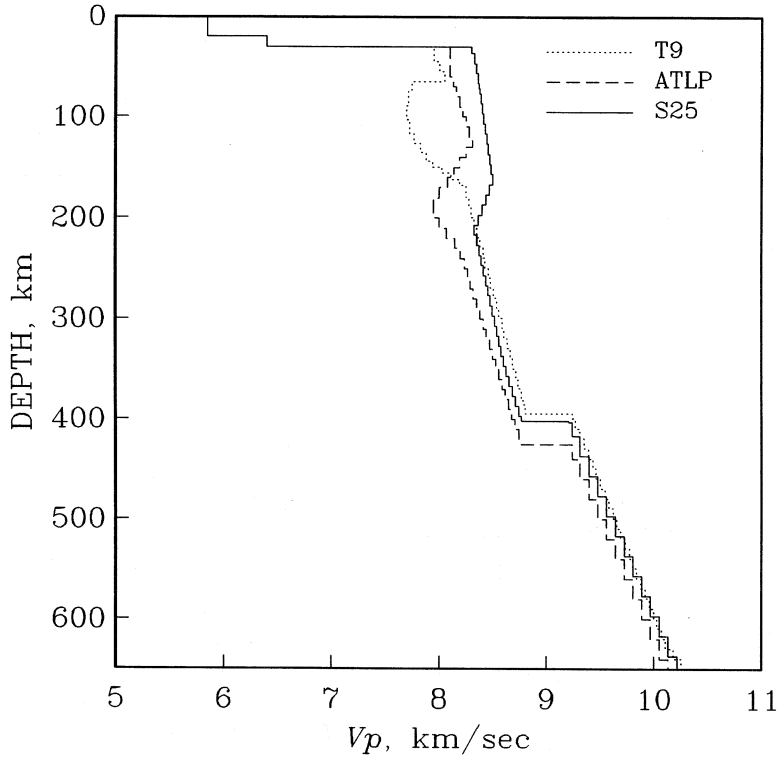

Fig. 2. Velocity models derived by several authors for different tectonic provinces: T9 has been obtained by Burdick (1981) for the West Mediterranean basin; ATLP by Zhao and Helmberger (1993) for the Northwest Atlantic Ocean; S25 by LeFevre and Helmberger (1989) for the Canadian shield.

After some testing, a simple triangular source time function has been used for all the events, with 1 s rise time and 1 s falloff time. The appropriate WWSSN-LP instrument response and a Futtermann attenuation operator (Futtermann, 1962) have been used respectively for $I(t)$ and $A(t)$. The Futtermann attenuation operator is a function of $t* = (T/Q)$, where T is the travel time and Q is an average of the quality factor along the ray path; an exact computation of synthetic waveforms would require the use of the proper $t*$ for each ray path, but Burdick and Helmberger (1978) demonstrated that no significative difference results from constructing synthetic seismograms by summing the contribution of rays computed either with a single averaged $t*$ or each one with its own $t*$. Moreover, in this case there is no sufficient information to determine a reliable model for the anelastic attenuation. A technique based on the Cagniard-de Hoop method (Helmberger, 1983) has been applied to compute Green's functions. This procedure allows more accurate computations of body wave synthetic seismograms in horizontally layered media with respect to the WKBJ method (Chapman, 1978): Grand and Helmberger (1984) and LeFevre and Helmberger (1989) pointed out some non realistic feature resulting in WKBJ synthetic seismogram computation.

From previously mentioned tomographic studies it follows that the degree of vertical heterogeneity is likely to be much higher than the horizontal one such that, at a regional scale, the area could be treated as laterally homogeneous, at least in first approximation. Because of the source locations, structural variation could be expected for different paths. This possibility has been investigated by calibrating the velocity structure to model the propagation paths for events 1 at TOL, MAL and PTO, that are comprised in a narrow angle, and then the result has been tested for the other paths.

In order to get first order information on the compressional velocity structure, synthetics have been computed by using published models which are appropriate for different tectonic regions (fig. 2). S25 was obtained by LeFevre and Helmberger (1989) for the Eastern Canada and is characteristic of stable continental regions; ATLP was recently obtained by Zhao and Helmberger (1993) for the upper mantle structure beneath the Northwestern Atlantic Ocean and is appropriate for regions having an old oceanic crust (70 to 150 Ma); T9, which is typical for a tectonic region, was used by Burdick (1981) to model North Aegean earthquakes recorded in Spain (approximately the same area of this study). The main differences between these models are relative to the upper 400 km. In particular, the lid thickness and a differently pronounced low-velocity zone are the most striking features characterizing each model. The different signatures of such features on travel times and amplitudes of the triplications can clearly be seen in the waveforms.

Figure 3 shows the comparison between data and synthetics computed with the different velocity models S25, ATLP and T9. It should be noticed that waveforms have been shifted along the time axes in order to align the first arrival. Since no reliable information on the crustal structure is available in these areas, an identical simplified model for the crust has been used in all the models; as a consequence, attention has been mainly focused on relative timing and amplitudes rather than on absolute travel times. For the sake of completeness, note that travel times predicted by S25 and T9 are respectively too small and too large, while ATLP gives, on average, travel times which are in good agreement (differences are less than 5 s) with the observed ones.

As previously noticed, these models do not have dramatic differences below 400 km; around this depth a strong velocity discontinuity (about 5%) is present. This velocity increase is responsible for a later phase, indicated by arrows in the figure, also observed in the data. It is evident that the model T9 is inadequate to describe this

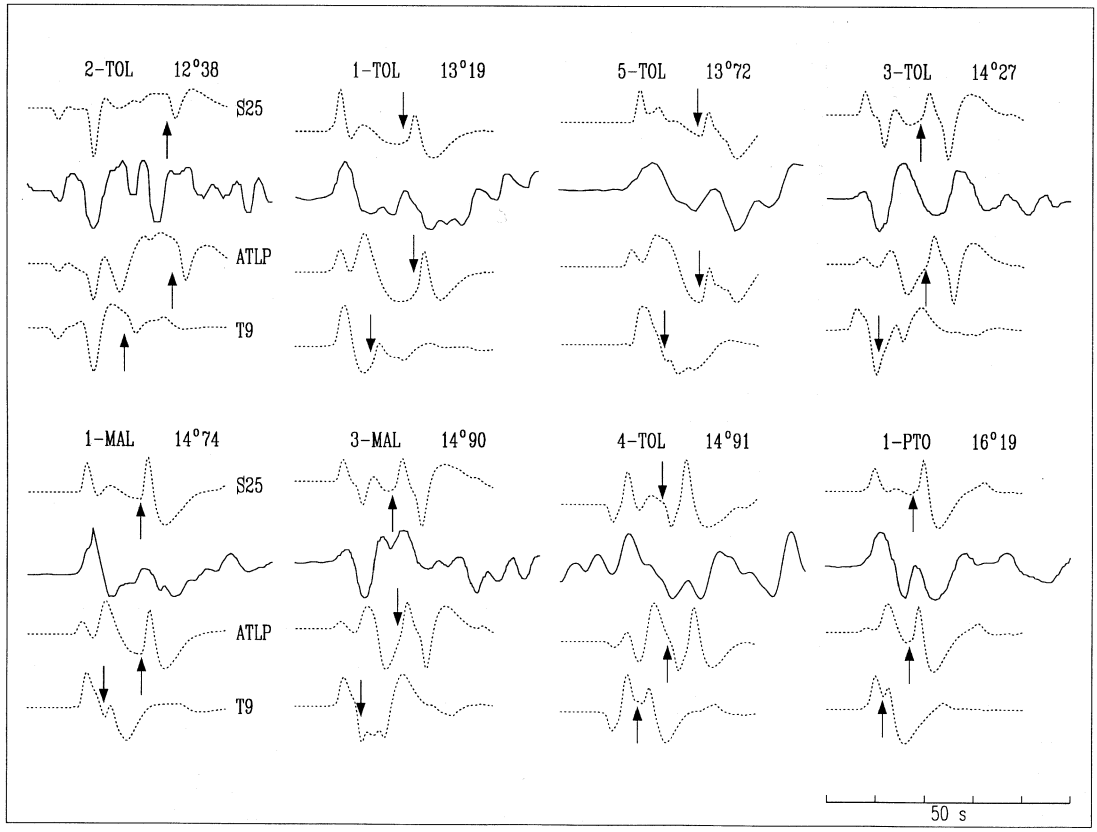

Fig. 3. Comparison between WWSSN-LP waveforms and synthetic seismograms computed for the velocity models shown in fig. 2. The number before the station name identifies the event, according to the map in fig. 1. The epicentral distances are also indicated. The arrows denote the arrivals associated with the reflection from the velocity discontinuity located at about 400 km depth.

feature. In fig. 4 the triplication curves for T9 and S25 are compared. For distances less than 18°, C-A travel times are always larger for stable continental structures than for tectonic ones. Because of the presence of a thin lid and a pronounced low-velocity zone, first arrivals for T9 (A branch) are formed by phases bottoming in the upper mantle below the asthenosphere, while lithospheric phases are predicted for S25; since rays bottoming at shallow depth have longer paths in the low velocity zone than those reflected from the «400 km discontinuity», the lower is the velocity in the asthenosphere the smaller are C-A times. Too sharp peaks and large C-A times are predicted by S25. The double arrival before the 400 km reflection in ATLP synthetics is formed by lid phases (P_n) followed by energy bottoming below 200 km (A branch), where velocity has a high gradient (see fig. 2); the delay between the arrivals is controlled by the thickness and velocity distribution in the low velocity layer. This feature is occasionally observed in the data selected for this study. On the whole, syn-

Table II. WMP model.

Depth	Velocity	Depth	Velocity	Depth	Velocity
20	5.85	170	8.10	398	8.78
30	6.40	180	8.11	405	8.80
40	7.91	190	8.12	415	8.90
50	8.00	198	8.13	435	9.00
60	8.06	208	8.16	465	9.20
70	8.12	218	8.19	487	9.26
80	8.13	248	8.20	527	9.50
100	8.14	258	8.22	537	9.52
120	8.15	298	8.25	547	9.52
130	8.16	313	8.26	557	9.54
140	8.02	368	8.35	577	9.58
150	8.04	378	8.58	597	9.62
160	8.08	388	8.68	617	9.80

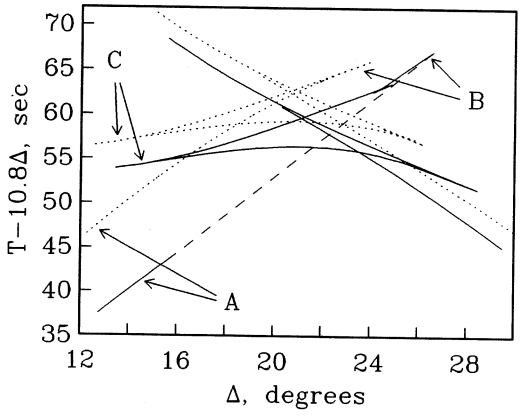

Fig. 4. Triplication curves generated by T9 (dotted) and S25 (solid). Letters individuate the different branches of the first triplication. The dashed segment on the S25 triplication curve has been interpolated because, for this model, the branch AB has a shadow zone between 16° and 26°.

thetics for ATLP better approximate the observed waveforms with respect to the other two models; however, it should be noticed that none of the models is able to predict any other phase.

On these grounds, some conclusions about the upper mantle structure of the area under study could already be drawn: a) a not-too-thin lid seems to be present; b) a low-velocity layer is suggested by some data; c) the low-velocity layer cannot be too slow or too thick; d) some complexity has to be present between 200 and 400 km.

4. Results and discussion

According to the results obtained by comparing observed with synthetic seismograms computed for the three considered models, a new model has been developed and then refined by a trial-and-error approach. Figure 5 shows the comparison between data and synthetic seismograms computed using the velocity structure shown in table II. The quality of the fits is excellent, particularly for 1-TOL, 1-MAL, 5-TOL and 3-MAL (event number-station name); in most cases minor features of the seismograms are also reproduced. The new model, WMP, is illustrated in fig. 6, together with S25, T9 and ATLP. WMP is very similar to ATLP within the lid, while the low velocity zone is less prominent. At

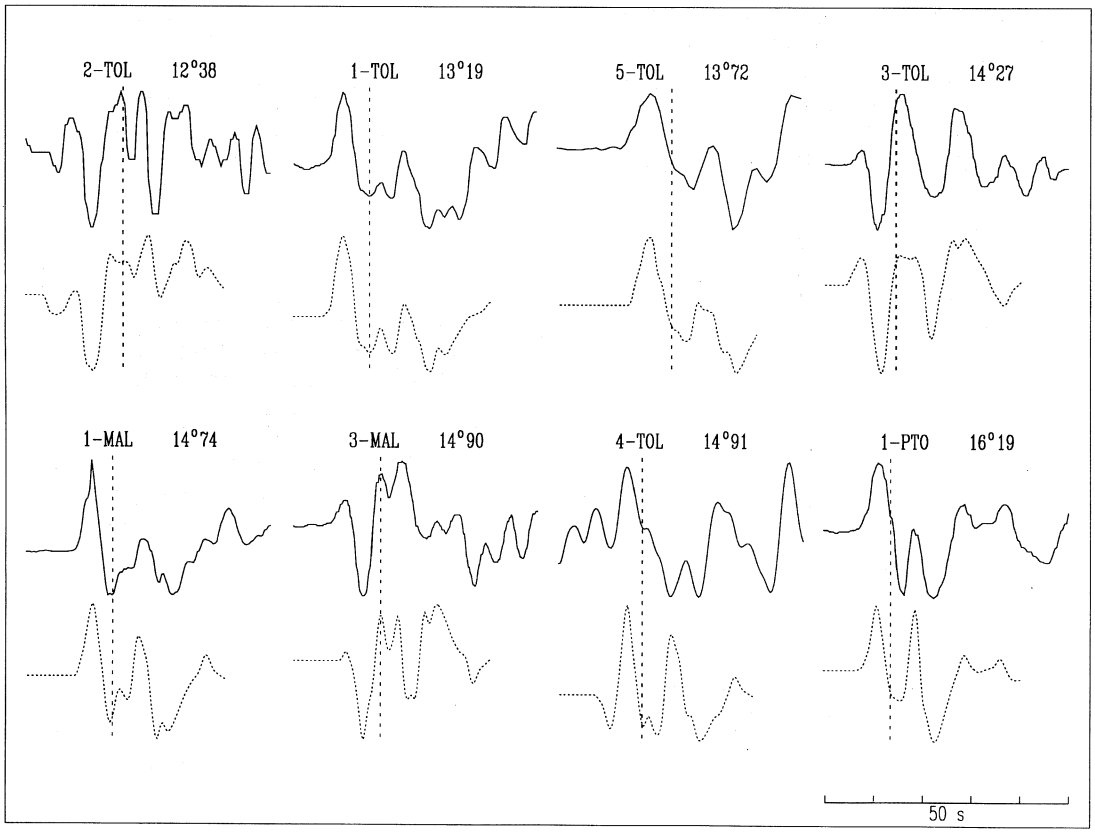

Fig. 5. Comparison of WWSSN-LP waveforms with synthetic seismograms computed by using the model derived in this study (WMP). The vertical dashed bars mark the phase generated by the «313 km discontinuity».

intermediate depths (200-400 km) the velocity gradient is much lower than the other models and the «400 km discontinuity» has been raised to 370 km.

Even though the fit for 4-TOL has been sensibly improved with respect to the other models, not negligible differences between data and synthetics still remain for this earthquake that need to be discussed. Event 4 is located in the Apennines, not far from events 1 and 5; its source-to-receiver distance is about the same of 1-MAL and 3-MAL and nevertheless, this is the only waveform displaying a clear difference between data and synthetics, even though the timing of the phases appears to be right. Following these considerations, this misfit has been imputed to an error in the source mechanism. Some attempt has been made to determine better fitting source parameters, but with no success.

Although WMP provides very good fits, some discussion is needed on the degree of approximation since it is not possible to give a quantitative estimation of the resolution for forward modeling.

From the previous section it follows that the features of the shallower phases, arriv-

ing first at regional distances, are controlled by the thickness and velocity distribution of the lid and the low-velocity zone. In order to get a detailed and well constrained model for the uppermost 200 km in the mantle, good quality recordings at epicentral distances shorter than 10°-12° would be particularly suitable. But, due to their scarce occurrence in the Western Mediterranean basin and to the presence of strong long-period lithospheric phases (*PL* phase) in these waveforms, no fine modeling is presently possible for the shallow depths. On the other hand, a-d) requirements derived in the previous section strongly restrict the domain of the possible solutions in the model space. In fact, very different starting models have been adopted so that several families have been generated. Due to the use of a very fast code to compute synthetics, a very large number of models (>2000) have been tested. Even relaxing the mentioned restrictions, the better fitting models were always very similar to WMP.

As far as the depths between 200 km and 400 km are concerned, it is remarkable that, unlike S25, T9 and ATLP, WMP is able to predict, in addition to the correct relative timing and amplitude ratio of the two major phases, also the complexities of the waveforms produced at intermediate depths. In particular, at the time indicated by the vertical bars in fig. 5, a distinct arrival is observed in all the data. Since different stations and events with different epicentral locations, depth and mechanism have been considered, this phase cannot be

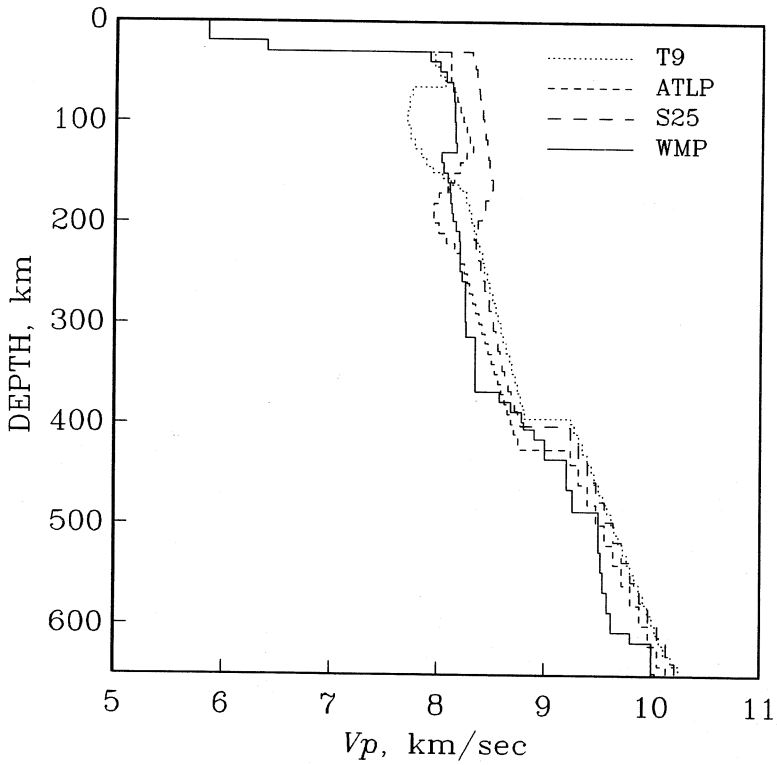

Fig. 6. The compressional velocity model WMP, derived in this study, compared with T9, ATLP and S25.

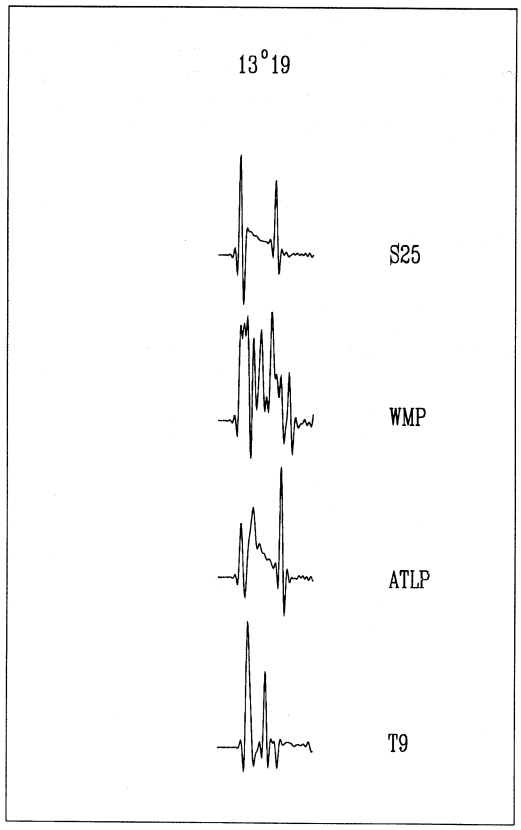

Fig. 7. Response functions for models S25, WMP, ATLP and T9. The responses have been low pass filtered to remove the noise due to model layering.

interpreted as an effect due to the source or to the local structure: its occurrence is likely to be due to a deep structural feature. From this study, it is consistent with a reflected phase from a 1% velocity discontinuity located at 313 km depth. The velocity above this interface is constrained by the modeling of the event 1 at TOL, MAL and PTO; modeling the same event prevents misinterpretations due to variation of source depth and mechanism that may lead to incorrect phase timing. Moreover, the stations are located at a narrow angle, such that no very different paths are involved. A very slow velocity (V_p = 8.26 km/s) has been found at this depth. The velocity below the interface has been obtained by matching the amplitude of the reflected phase. It is worthwhile to notice that, through fine modeling of long period waveforms, a velocity discontinuity as small as 1% has been detected.

Unusual features have been found for the discontinuity responsible for the first triplication. Several authors obtained a depth of 400 km for this interface and a very sharp velocity discontinuity (about 5%). In this study, no evidence for such a high jump has been found; on the contrary, an abrupt increase in the velocity gradient starting with a small discontinuity located at 370 km depth resulted from modeling. Like for the 313 km discontinuity, the velocity above this transition layer has been constrained by modeling a single event at all the stations. This velocity was also found to be smaller (Vp = 8.35 km/s) than the values usually reported for these depths.

It is important to notice that no adjustments seem to be needed for the single paths: a single model has been used for all the events. This is an indication that no major lateral variations are present perpendicular to the paths, at least for large depths. Some lateral heterogeneity may exist at depth shallower than 200 km, as is expected for event 3, which is located in the Southern Tyrrhenian Sea, but it does not seem to produce strong effect on seismograms; only a minor misfit for this event is detectable for TOL and might actually be explained with the presence of the subducting slab that perturbs the wavefield.

Several tests have been performed to investigate the reliability of WMP with regard to depths and absolute velocity values of the 313 km interface and the 400 km transition layer: it resulted that changes as small as 5 km for depths and 0.05 km/s for velocities would produce significative differences in the waveforms.

In order to get an idea of the complexities that can be predicted by the different

velocity models, the response functions for the models shown in fig. 6, computed for a distance of 13°19 (corresponding to 1-TOL), are shown in fig. 7. It is evident that S25, T9 and ATLP have been constructed especially to match the two most important phases observed in the data and no energy at all is predicted between them. On the other hand, WMP provides such a complex response function that it is almost impossible to individuate the strongest phases.

5. Conclusions

Once again waveform modeling has proved to be a powerful tool for providing detailed structural information. In this paper an attempt to finely model the data has been made and the results appear to be promising. Although paths through a very complex tectonic environment have been considered, detailed information have been obtained, especially on the deep structure of the upper mantle. With the recent progress in broad-band seismology and, in particular, with the commitment undertaken by several instrumentation programs (such as MEDNET, NARS but also global network like GEOSCOPE and IRIS/GSN) more data of high quality are expected to be collected, providing the base for further analysis.

Unlike previous analogous studies performed in the area, a not very pronounced low-velocity zone and a 100 km thick lid have been found. These features are similar to those typical for an old ocean structure found in the West Atlantic Ocean by Grand and Helmberger (1984) and Zhao and Helmberger (1993) by using respectively *S* and *P* body waves.

Acknowledgements

I am grateful to D. V. Helmberger, who introduced me to the study of upper mantle, and to A. Morelli for his encouragement (pressure) in writing this paper. Discussions with Salvatore Mazza, who also helped in plotting the figures, and criticisms from M. Cocco, D. Giardini and A. Zollo contributed to this paper.

REFERENCES

AMATO, A., B. ALESSANDRINI and G.B. CIMINI (1993): Teleseismic wave tomography of Italy, in *Seismic tomography: theory and methods*, edited by H.M. IYER and K. HIRAHARA (Chapman and Hall, London), 361-397.

ANDERSON, D.L. and J.D. BASS (1984): Mineralogy and composition of the upper mantle, *Nature*, **320**, 321-328.

ANDERSON, H. and J. JACKSON (1987a): The deep seismicity of the Tyrrhenian Sea, *Geophys. J. R. Astr. Soc.*, **91**, 613-637.

ANDERSON, H. and J. JACKSON (1987b): Active tectonics of the Adriatic region, *Geophys. J. R. Astr. Soc.*, **91**, 937-984.

BURDICK, L.J. (1981): A comparison of upper mantle structure beneath North America and Europe, *J. Geophys. Res.*, **86**, 5926-5936.

BURDICK, L.J. and D. V. HELMBERGER (1978): The upper mantle *P* velocity structure of the Western United States, *J. Geophys. Res.*, **83**, 1699-1712.

CARA, M., A. NERCESSIAN and G. NOLET (1980): New inferences from higher mode data in Western Europe and Northern Eurasia, *Geophys. J. R. Astr. Soc.*, **61**, 459-478.

CHAPMAN, C.H. (1978): A new method for computing synthetic seismograms in laterally homogeneous media, *Geophys. J. R. Astr. Soc.*, **54**, 481-518.

DUFFY, T.S. and D.L. ANDERSON (1989): Seismic velocities in mantle minerals and the mineralogy of the upper mantle, *J. Geophys. Res.*, **94**, 1895-1912.

ENGLAND, P.C. and M.H. WORTHINGTON (1977): The travel time of *P* seismic waves in Europe and Western Russia, *Geophys. J. R. Astr. Soc.*, **48**, 63-70.

FUTTERMANN, W. I. (1962): Dispersive body waves, *J. Geophys. Res.*, **67**, 5279-5291.

GRAND, S.P. and D. V. HELMBERGER (1984): Upper mantle shear structure beneath the Northwest Atlantic Ocean, *J. Geophys. Res.*, **89**, 11465-11475.

HAGER, B.H. (1984): Subducted slabs and the geoid: constraints on the mantle rheology and flow, *J. Geophys. Res.*, **89**, 6003-6015.

HELMBERGER, D. V. (1972): Long period body wave propagation from 4° to 13°, *Bull. Seismol. Soc. Am.*, **62**, 325-341.

HELMBERGER, D.V. (1983): Theory and application of synthetic seismograms, in *Proceedings of the International School of Physics «Enrico Fermi», LXXXV Course, Earthquake: Observations, The-*

ory and Interpretation, edited by H. KANAMORI and E. BOSCHI (North Holland), 174-222.

ITA, J. and L. STIXRUDE (1992): Petrology, elasticity and composition of the mantle transition zone, *J. Geophys. Res.*, **97**, 6849-6866.

LEFEVRE, L. V. and D.V. HELMBERGER (1989): Upper mantle *P* velocity of the Canadian shield, *J. Geophys. Res.*, **94**, 17749-17765.

MACDONALD, G.J.F. (1963): The deep structure of continents, *Rev. Geophys.*, **1**, 587-665.

MARILLIER, F. and ST. MUELLER (1985): The Western Mediterranean region as an upper-mantle transition zone between two lithospheric plates, *Tectonophysics*, **118**, 113-130.

MAYER-ROSA, D. and ST. MUELLER (1973): The gross velocity-depth distribution of *P*- and *S*-waves in the upper mantle of Europe from earthquake observations, *Z. Geophys.*, **39**, 395-410.

PANZA, G.F., ST. MUELLER and G. CALCAGNILE (1980): The gross features of the lithosphere-asthenosphere system in Europe from seismic surface waves and body waves, *Pure Appl. Geophys.*, **118**, 1209-1213.

PAULSSEN, H. (1987): Lateral heterogeneity of Europe's upper mantle as inferred from modelling of broad-band body waves, *Geophys. J. R. Astr. Soc.*, **91**, 171-199.

PAYO, G. (1969): Crustal structure of the Mediterranean Sea. Part II. Phase velocities and travel times, *Bull. Seismol. Soc. Am.*, **59**, 23-42.

ROMANOWICZ, B.A. (1980): A study of large-scale lateral variations of *P* velocity in the upper mantle beneath Western Europe, *Geophys. J. R. Astr. Soc.*, **63**, 217-232.

SCARPA, R. (1982): Travel time residuals and three-dimensional velocity structure of Italy, *Pure Appl. Geophys.*, **120**, 583-606.

SNIEDER, R. (1988): Large waveform inversions of surface waves for lateral heterogeneity-2. Application to surface waves in Europe and the Mediterranean, *J. Geophys. Res.*, **93**, 12067-12080.

SPAKMAN, W. (1991): Delay-time tomography of the upper mantle below Europe, the Mediterranean, and Asia minor, *Geophys. J. Int.*, **107**, 309-332.

SPAKMAN, W., M.J.R. WORTEL and N.J. VLAAR (1988): The Hellenic subduction zone: a tomographic image and its geodynamic implications, *Geophys Res. Lett.*, **16**, 1097-1100.

WALCK, M.C. (1984): The *P*-wave upper mantle structure beneath an active spreading center: the Gulf of California, *Geophys. J. R. Astr. Soc.*, **76**, 697-723.

ZHAO, L.S. and D.V. HELMBERGER (1993): Upper mantle compressional velocity structure beneath the Northwest Atlantic Ocean, *J. Geophys. Res.*, **98**, 14185-14196.

(received November 16, 1993;
accepted February 9, 1994)